

# DRL-Based Beam Positioning for LEO Satellite Constellations with Weighted Least Squares

Po-Heng Chou<sup>1</sup>, Chiapin Wang<sup>2</sup>, Kuan-Hao Chen<sup>2</sup>, and Wei-Chen Hsiao<sup>2</sup>

<sup>1</sup>Research Center for Information Technology Innovation (CITI), Academia Sinica (AS), Taipei 11529, Taiwan

<sup>2</sup>Department of Electrical Engineering, National Taiwan Normal University (NTNU), Taipei 106308 Taiwan

E-mails: d00942015@ntu.edu.tw, chiapin@ntnu.edu.tw, 61375063h@ntnu.edu.tw, 61275046h@ntnu.edu.tw

**Abstract**—This paper investigates a lightweight deep reinforcement learning (DRL)-assisted weighting framework for CSI-free multi-satellite positioning in LEO constellations, where each visible satellite provides one serving beam (one pilot response) per epoch. A discrete-action Deep Q-Network (DQN) learns satellite weights directly from received pilot measurements and geometric features, while an augmented weighted least squares (WLS) estimator provides physics-consistent localization and jointly estimates the receiver clock bias. The proposed hybrid design targets an accuracy-runtime trade-off rather than absolute supervised optimality. In a representative 2-D setting with 10 visible satellites, the proposed approach achieves sub-meter accuracy (0.395m RMSE) with low computational overhead, supporting practical deployment for resource-constrained LEO payloads.

**Index Terms**—LEO satellites, reinforcement learning, satellite weighting, WLS positioning, NTN.

## I. INTRODUCTION

The integration of terrestrial, aerial, and satellite segments into a unified ground-air-space architecture has emerged as a key enabler for future sixth-generation (6G) networks, promising seamless connectivity, low latency, and global coverage [1]. Among these, low Earth orbit (LEO) satellite constellations are particularly attractive due to their wide coverage, rapid revisit capability, and suitability for delay-sensitive services. However, their highly dynamic topology, interference-prone links, and constrained on-board processing capabilities present significant challenges for robust and energy-efficient service delivery [1]–[3].

Recent research has addressed these challenges from multiple perspectives. A Lyapunov-based beam management strategy was developed for LEO networks with random traffic arrivals and time-varying topologies, effectively reducing beam revisit times and handover frequency [2]. A multi-satellite beam-hopping framework was introduced to balance load and avoid interference in non-geostationary orbit (NGSO) constellations, significantly improving spectral efficiency [4]. Deep reinforcement learning (DRL)-driven handover protocols have been designed to eliminate measurement-report overhead, thereby reducing access delay and collision rates in regenerative-type LEO networks [5]. Cooperative beam scheduling and beamforming approaches in multi-beam LEO systems have shown positioning accuracy gains of up to

17.1% under Cramér-Rao lower bound (CRLB) criteria [6]. Reinforcement learning-based robust beamforming methods for multibeam downlinks have also demonstrated resilience to imperfect channel knowledge [7]. In addition, cooperative beam-hopping control strategies in ultra-dense LEO constellations have been proposed to enhance time-difference-of-arrival (TDOA) positioning performance [8].

Beyond the physical layer, system-level frameworks have also been explored. A symbiotic radio approach using collaborative DRL has been proposed for intelligent resource optimization in non-terrestrial networks (NTNs) [3]. Standardization and system-level research on integrated terrestrial and non-terrestrial networks (TN-NTN) localization have highlighted key challenges in synchronization, interference, and robustness [1]. Moreover, federated learning frameworks have been investigated for NTNs to enhance scalability and privacy in multi-tier deployments [9].

Despite these advances, most existing solutions still rely heavily on explicit channel state information (CSI) or involve computationally intensive optimization, limiting real-time applicability for resource-constrained LEO platforms. Traditional statistical estimation methods, such as weighted least squares (WLS) [10], widely used in positioning problems, provide reliable accuracy but lack adaptability in dynamic multi-satellite environments with heterogeneous link qualities. Meanwhile, DRL has proven effective in sequential decision-making tasks [11], yet its integration with lightweight positioning remains underexplored in NTNs.

Motivated by these gaps, this work extends the use of DRL beyond prior studies that focused primarily on handover optimization [5], load-balanced beam hopping [4], or cooperative scheduling [6]. We adopt the DQN framework [11], which approximates the action-value function with deep neural networks to enable efficient decision-making in large state-action spaces. Unlike previous DRL approaches requiring explicit CSI or heavy network coordination, the proposed framework applies DQN for multi-satellite positioning in multiple-input multiple-output (MIMO) LEO systems and integrates it with a WLS estimator [10]. This design allows adaptive beam selection and weighting directly from received pilot measurements. Thus, it eliminates explicit CSI estimation, achieving robustness under interference-prone and global navigation satellite system (GNSS)-denied conditions. In addition, it significantly reduces computational complexity compared to conventional optimization or deep learning baselines. While

This work was supported in part by the National Science and Technology Council (NSTC) of Taiwan under Grant 113-2926-I-001-502-G and 114-2221-E-003-033.

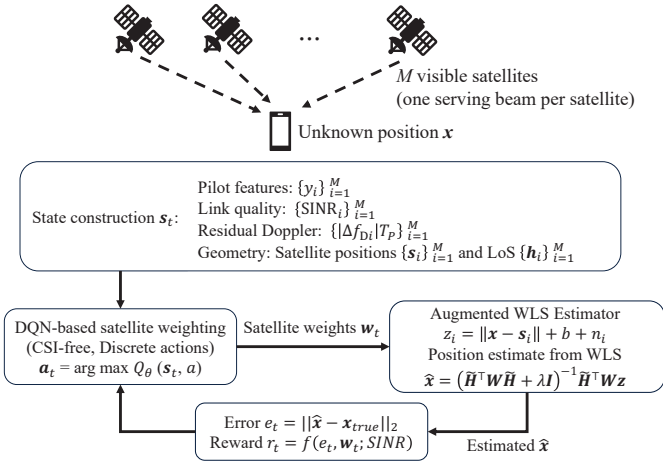


Fig. 1: System overview of the proposed CSI-free DQN-WLS multi-satellite positioning framework.

CRLB-based optimization offers theoretical bounds, it is analytically intractable for fast-varying satellite geometry. Hence, an augmented WLS estimator is adopted, whose efficiency asymptotically approaches the CRLB under Gaussian noise.

The main contributions of this paper are summarized as follows:

- **CSI-free, lightweight hybrid design:** We couple a discrete-action DQN *satellite-weighting* policy with an augmented WLS solver to enable CSI-free multi-satellite positioning, while maintaining a small on-board inference footprint.
- **Deployment-oriented action parameterization:** We design a quantized *satellite-weight* action space compatible with practical on-board control granularity, improving numerical robustness of the downstream WLS inversion while remaining tractable for DQN training.
- **Accuracy-runtime evidence and insight:** We provide a comparative evaluation highlighting the trade-off between positioning accuracy and computational cost across representative baselines, illustrating the regime where the proposed approach is attractive for real-time LEO operation.

## II. SYSTEM MODEL

Fig. 1 illustrates the proposed CSI-free multi-satellite positioning pipeline. At each epoch,  $M$  visible LEO satellites are available, and each satellite schedules one serving beam to deliver a pilot observation. Pilot-derived features  $\{y_i\}_{i=1}^M$ , geometry information (e.g.,  $\{s_i, h_i\}$ ), and the normalized residual Doppler magnitudes  $\{|\Delta f_{D_i}|T_p\}_{i=1}^M$  (with  $T_p$  defined in (8)) constitute the DQN state. The DQN selects a discrete action that is mapped to a normalized satellite-weight vector, which is then applied to the augmented WLS estimator to jointly estimate the UT position and the receiver clock bias.

### A. Coordinate System and Satellite geometry

We consider  $M$  visible LEO satellites from a constellation. Let  $\{s_i\}_{i=1}^M$  denote the satellite positions in the earth-

centered, earth-fixed (ECEF) coordinate system within a short observation window. The unknown UT position is denoted by  $\mathbf{x} \in \mathbb{R}^{d \times 1}$ .

For satellite  $i$ , the line-of-sight (LoS) unit vector from the satellite to the UT is

$$\mathbf{h}_i \triangleq \frac{\mathbf{x} - \mathbf{s}_i}{\|\mathbf{x} - \mathbf{s}_i\|}, \quad i = 1, \dots, M. \quad (1)$$

where  $\mathbf{h}_i \in \mathbb{R}^{d \times 1}$  and  $d = 2$  or  $3$  depending on the positioning dimension. The satellite geometry  $\{s_i, h_i\}$  is assumed quasi-static within a 1 to 5 s window, updated by ephemeris and the scheduler.

### B. Channel Model

Following the model in [6], the narrowband line-of-sight (LoS) channel between the satellite and the UT is dominated by a single deterministic path. Let  $\mathbf{s}_i \in \mathbb{R}^3$  denote the satellite antenna phase-center position and  $d_i = \|\mathbf{x} - \mathbf{s}_i\|$  the slant range between satellite  $i$  and the UT. Consider a uniform planar array (UPA) [13] with  $N_x \times N_y$  elements and total antenna count  $N = N_x N_y$ . The complex baseband channel vector from satellite  $i$  is expressed as

$$\mathbf{g}_i = \beta_i e^{j\phi_i} \mathbf{a}_t(\varphi_i) \in \mathbb{C}^{N \times 1}, \quad (2)$$

where  $\phi_i$  denotes the random phase uniformly distributed in  $[0, 2\pi)$ ,  $\mathbf{a}_t(\varphi_i)$  is the UPA transmit steering vector at the departure angle  $\varphi_i$ , and  $\beta_i$  represents the large-scale channel gain defined as

$$\beta_i = \sqrt{\frac{G_t G_r}{L_i}}, \quad L_i = \left( \frac{4\pi f_c d_i}{c} \right)^2, \quad (3)$$

with  $f_c$  denoting the carrier frequency,  $c$  the speed of light, and  $G_t, G_r$  the transmit and receive antenna gains, respectively. The transmit steering vector  $\mathbf{a}_t(\varphi_i)$  follows a standard  $N_x \times N_y$  UPA response model [13]. To reduce exposition, we omit its element-wise expression and directly use  $\mathbf{a}_t(\varphi_i)$  to compute the effective beamformed gain  $|\mathbf{g}_i^H \mathbf{f}_i|^2$  in (5).

Within each epoch, the UT correlates  $N_p$  received pilot samples to obtain one scalar pilot feature per satellite:

$$y_i \triangleq \frac{1}{N_p} \sum_{n=0}^{N_p-1} r[n] x_i^*, \quad (4)$$

where  $r[n]$  denotes the received pilot sample and  $x_i$  is the known pilot symbol of satellite  $i$ . After ephemeris-based Doppler pre-compensation, the residual Doppler is modeled as  $\Delta f_{D_i} \sim \mathcal{N}(0, \sigma_{\Delta f_D}^2)$ , i.i.d. across satellites and epochs.

Accordingly, we compute the instantaneous power-domain link-quality metric under frequency reuse as

$$\text{SINR}_i = \frac{|\mathbf{g}_i^H \mathbf{f}_i|^2}{\sum_{k \neq i} |\mathbf{g}_k^H \mathbf{f}_k|^2 + \sigma^2}, \quad (5)$$

where the summation term accounts for *frequency-reuse co-channel beams* transmitted by other satellites on the same time-frequency resource, and  $\mathbf{g}_k$  denotes the channel vector from satellite  $k$  to the UT within the considered epoch.

The residual Doppler impact is incorporated via an equivalent measurement-reliability penalty in (7)-(8). We emphasize that a full orthogonal frequency-division multiplexing (OFDM) inter-carrier interference (ICI) treatment is beyond the scope of this work and can be captured by an equivalent SINR/variance penalty when needed. The instantaneous per-satellite link-quality metric  $\text{SINR}_i$  under frequency reuse computed from (2)-(5) is normalized to  $[0, 1]$  and later used as part of the DRL observation vector.

### C. Observation Model

In conventional multi-satellite positioning, the UT location is inferred from multiple range-like measurements collected from visible satellites. To build a unified and analytically tractable model, we define a set of differentiable measurements  $\mathbf{z} \in \mathbb{R}^M$  that depend on the geometric distances between  $\mathbf{x}$  and the satellite positions  $\{\mathbf{s}_i\}$ . For satellite  $i$ , a pseudorange-like measurement is modeled as

$$z_i = \|\mathbf{x} - \mathbf{s}_i\| + b + n_i, \quad (6)$$

where  $b$  is the receiver clock bias and  $n_i \sim \mathcal{N}(0, \sigma_i^2)$  is zero-mean Gaussian noise whose variance reflects the effective link quality of satellite  $i$ . To incorporate residual Doppler, we model an equivalent reliability penalty on the range-like measurement. Specifically, we define an *effective* SINR as

$$\text{SINR}_i^{\text{eff}} = \frac{\text{SINR}_i}{1 + \kappa (|\Delta f_{D_i}| T_p)^2}, \quad (7)$$

where  $\kappa$  is a scaling parameter controlling the Doppler-induced reliability penalty. The measurement noise variance is modeled as

$$\sigma_i^2 = \frac{\sigma_0^2}{\text{SINR}_i^{\text{eff}}}, \quad T_p = N_p T_s, \quad (8)$$

where  $\sigma_0^2$  is a nominal noise level,  $\kappa$  controls the Doppler-induced penalty strength, and  $T_p$  denotes the pilot integration time used for pilot correlation/averaging within one epoch. This model captures that residual Doppler degrades pilot correlation quality and thus reduces the reliability of range-like measurements, which is directly reflected in the WLS weighting.

Linearizing the pseudorange-like measurements in (6) at a reference  $\mathbf{x}_0$  yields

$$\mathbf{z} \approx \mathbf{H}\mathbf{x} + b\mathbf{1} + \mathbf{n}, \quad (9)$$

where the  $i$ -th row of  $\mathbf{H} \in \mathbb{R}^{M \times d}$  is  $\mathbf{h}_i^\top$  defined in (1),  $\mathbf{1} \in \mathbb{R}^{M \times 1}$ , and  $\mathbf{x}_0$  is an initial position estimate.

### D. Augmented Weighted Least Squares (WLS)

Let  $\tilde{\mathbf{H}} = [\mathbf{H} \ \mathbf{1}] \in \mathbb{R}^{M \times (d+1)}$  and  $\tilde{\mathbf{x}} = [\mathbf{x}^\top \ b]^\top$ . Given  $\mathbf{W} = \text{diag}(w_1, \dots, w_M)$ , the augmented WLS estimate is

$$\hat{\tilde{\mathbf{x}}} = (\tilde{\mathbf{H}}^\top \mathbf{W} \tilde{\mathbf{H}} + \lambda \mathbf{I})^{-1} \tilde{\mathbf{H}}^\top \mathbf{W} \mathbf{z}, \quad (10)$$

with ridge parameter  $\lambda > 0$  for numerical stability. We then parse  $\hat{\mathbf{x}}$  and  $\hat{b}$  from  $\hat{\tilde{\mathbf{x}}}$ .

## III. PROBLEM FORMULATION

From the system model above, the WLS estimator in (10) computes the UT position  $\hat{\mathbf{x}}$  based on the satellite weight vector  $\mathbf{w} = [w_1, \dots, w_M]^\top$ . The instantaneous positioning error is defined as

$$e = \|\hat{\mathbf{x}} - \mathbf{x}_{\text{true}}\|_2. \quad (11)$$

The objective of the multi-satellite positioning problem is to find the optimal weight vector  $\mathbf{w}^*$  that minimizes the expected positioning error:

$$\mathbf{w}^* = \arg \min_{\mathbf{w} \in \mathcal{W}} \mathbb{E}[\|\hat{\mathbf{x}}(\mathbf{w}) - \mathbf{x}_{\text{true}}\|_2^2], \quad (12)$$

subject to  $w_i \in [0, 1]$  and  $\sum_i w_i = 1$ , where  $\mathcal{W}$  denotes the feasible set of normalized weight vectors.

The above optimization is nonlinear and highly dependent on the satellite geometry through the matrix  $\mathbf{H}$  in (9). Since  $\mathbf{H}$  varies rapidly with satellite motion and the time-varying set of visible/serving satellite links, solving (12) analytically or by exhaustive search is computationally prohibitive. Conventional heuristic methods assign fixed or power-based weights that cannot adapt to dynamic link conditions.

To overcome these limitations, we reformulate the satellite-weight optimization as a sequential decision-making problem, where an agent learns to adjust  $\mathbf{w}$  based on observed satellite-link features and positioning feedback. This motivates the proposed DRL approach detailed in Section IV. To support practical deployability and numerical stability, the continuous weight vector is quantized into a finite action set: (i) it matches hardware-friendly weight granularity (e.g., codebook-like control), (ii) it mitigates ill-conditioning in the augmented WLS inversion under noisy beams, and (iii) it yields a tractable discrete action space for DQN training.

## IV. DQN-WLS BASED MULTI-SATELLITE POSITIONING

In this section, we present a DRL framework that integrates a DQN with a WLS estimator for accurate and adaptive multi-satellite positioning in LEO satellite systems. Unlike conventional geometry- or CSI-based methods, the proposed DQN-WLS scheme learns satellite-weighting strategies directly from received pilot measurements and geometric features, thus eliminating explicit CSI estimation and reducing computational complexity.

### A. Markov Decision Process Formulation

The beam-weight optimization problem in (12) is reformulated as a Markov decision process (MDP)  $\langle \mathcal{S}, \mathcal{A}, \mathcal{P}, \mathcal{R}, \gamma \rangle$ . At each discrete time step  $t$ , the environment (*BeamEnv*) generates a state vector  $\mathbf{s}_t \in \mathcal{S}$  that encapsulates both geometric and signal-level features of  $M$  visible satellite links. These include normalized satellite distances (or slant ranges), azimuth-elevation indicators, per-satellite SINR metrics, previous residual errors, and prior weight distributions.

**Action parameterization.** To comply with DQN's discrete-action setting, we quantize the continuous satellite weights into a finite action set constructed by top- $K$  satellite selections

and coarse weight levels  $\{0, 0.25, 0.5, 0.75, 1\}$ , followed by  $\ell_1$  normalization. Near-duplicate actions are pruned by correlation screening to keep the action set tractable.

The agent selects a discrete action  $a_t \in \mathcal{A}$ , which is mapped to a normalized weight vector  $\mathbf{w}_t$  applied to the WLS estimator. After performing the WLS estimation  $\hat{\mathbf{x}}_t$ , the environment computes the positioning error  $e_t = \|\hat{\mathbf{x}}_t - \mathbf{x}_{\text{true}}\|_2$  and generates a scalar reward  $r_t$  that reflects both accuracy and stability:

$$r_t = -\left(\frac{e_t}{\tau}\right)^2 - \alpha \sum_{i=1}^M w_{t,i} (1 - \text{SINR}_i^{\text{eff}}) - \beta (1 - \text{Entropy}(\mathbf{w}_t)), \quad (13)$$

where the entropy term is defined as

$$\text{Entropy}(\mathbf{w}_t) = -\sum_{i=1}^M w_{t,i} \log w_{t,i}, \quad (14)$$

which encourages exploration by promoting weight diversity. Here,  $\tau$  controls the error-scaling factor,  $\alpha$  penalizes low-quality satellite links, and  $\beta$  regulates the entropy contribution. The discount factor  $\gamma = 0.99$  encourages long-term optimization over sequential interactions.

### B. Network Architecture

The DQN approximates the action-value function  $Q_\theta(s, \mathbf{a})$  parameterized by  $\theta$ . The input layer concatenates per-satellite features with a total feature dimension  $F = 60$  for  $M = 10$  satellites. Two fully connected hidden layers of 128 neurons each, activated by ReLU, are used to extract latent geometric representations. After pruning redundant combinations, the discrete action set contains approximately  $10^2$  valid satellite-weight configurations. The network outputs  $|\mathcal{A}|$  Q-values over these quantized actions, and the selected action is mapped to a normalized weight vector  $\mathbf{w}_t$ .

To stabilize the subsequent WLS inversion, a ridge term  $\lambda \mathbf{I}$  is added to (10). The network parameters are initialized using He initialization, optimized via Adam with learning rate  $\eta = 10^{-3}$ , and updated using the Huber loss. A target network  $Q_{\bar{\theta}}$  is periodically synchronized with the main network  $Q_\theta$  every  $C = 200$  iterations to mitigate oscillations in temporal-difference targets.

### C. Training Procedure

During training, the agent interacts with the environment over multiple episodes. At each step  $t$ , the agent observes the current state  $s_t$ , selects an action  $\mathbf{w}_t = f_\theta(s_t)$  according to an  $\epsilon$ -greedy policy, applies  $\mathbf{w}_t$  to the WLS estimator, and receives a reward  $r_t$  and next state  $s_{t+1}$ . Each transition  $(s_t, \mathbf{w}_t, r_t, s_{t+1})$  is stored in a replay buffer  $\mathcal{D}$  of size  $10^4$ . Mini-batches of 32 samples are randomly drawn from  $\mathcal{D}$  to update the network parameters.

The target value for each sample is defined as

$$y_t = r_t + \gamma Q_{\bar{\theta}}(s_{t+1}, f_{\bar{\theta}}(s_{t+1})), \quad (15)$$

---

### Algorithm 1: DQN-WLS Based Satellite Positioning

---

**Input:** Environment BeamEnv, learning rate  $\eta$ , discount factor  $\gamma$ , target update interval  $C$ , exploration schedule  $\epsilon$

**Output:** Trained DQN policy  $\pi_\theta$  for adaptive beam-weighting

```

1 Initialize replay buffer  $\mathcal{D}$ , networks  $Q_\theta$  and target  $Q_{\bar{\theta}} \leftarrow Q_\theta$ ;
2 for  $episode = 1$  to  $E_{\text{max}}$  do
3   Reset environment and obtain initial state  $s_0$ ;
4   for each time step  $t$  do
5     Select action  $\mathbf{w}_t \leftarrow f_\theta(s_t)$  and apply  $\epsilon$ -greedy exploration;
6     Normalize  $\mathbf{w}_t$  s.t.  $\sum_i w_{t,i} = 1$ , form  $W_t = \text{diag}(\mathbf{w}_t)$ ;
7     Compute  $\hat{\mathbf{x}}_t$  via WLS in (10);
8     Compute positioning error  $e_t$  using (11);
9     Evaluate reward  $r_t$  via (13) and observe next state  $s_{t+1}$ ;
10    Store  $(s_t, \mathbf{w}_t, r_t, s_{t+1})$  in buffer  $\mathcal{D}$ ;
11    Sample mini-batch from  $\mathcal{D}$ ;
12    Compute target  $y_t$  using (15);
13    Update  $\theta \leftarrow \theta - \eta \nabla_\theta L_t(\theta)$  via Huber loss (16);
14    if  $\text{mod}(t, C) = 0$  then
15      | update target network  $Q_{\bar{\theta}} \leftarrow Q_\theta$ ;
16    end
17    if convergence or terminal state reached then
18      | break;
19    end
20  end
21 end
22 return Optimal policy  $\pi_\theta^*$  generating  $\mathbf{w}_t^*$  for each  $s_t$ 

```

---

and the temporal-difference (TD) loss follows the Huber formulation:

$$L_t(\theta) = \begin{cases} \frac{1}{2} \delta_t^2, & |\delta_t| < 1, \\ |\delta_t| - \frac{1}{2}, & \text{otherwise,} \end{cases} \quad (16)$$

where  $\delta_t = y_t - Q_\theta(s_t, \mathbf{w}_t)$ . Gradients are clipped with  $\|\nabla_\theta\| \leq 5$  to prevent divergence, and  $\epsilon$  decays exponentially from 1.0 to 0.01 during training. Convergence is typically achieved within 800 to 1000 episodes in the considered settings, after which the positioning error enters a stable sub-meter regime. Furthermore, the learned satellite weights exhibit interpretable behavior: high-SINR beams tend to receive larger weights, while redundant or correlated beams are automatically suppressed, indicating that the agent learns beam reliability from pilot-level observations without explicit CSI modeling.

## V. SIMULATION RESULTS AND ANALYSIS

### A. Experimental Setup

All simulations were conducted in Python using the PyTorch 2.5 framework on a workstation equipped with an Intel i9 CPU

and an NVIDIA RTX A6000 GPU. A 2-D coverage area of  $1000 \times 1000 \text{ m}^2$  is considered with  $M = 10$  visible satellites. The discount factor is set to  $\gamma = 0.99$ , the learning rate  $\eta = 10^{-3}$  (Adam optimizer), and the target network update interval  $C = 200$ . Each training episode consists of  $T = 100$  steps, and the replay buffer stores  $10^4$  transitions.

**Residual Doppler.** After ephemeris-based Doppler pre-compensation, the residual Doppler is modeled as a zero-mean Gaussian random variable with variance  $\sigma_{\Delta f_D}^2 = 5 \text{ (Hz}^2\text{)}$ , and its impact is incorporated into the measurement reliability via (7)–(8), where  $T_p = N_p T_s$ .

We compare six methods: PPO [14], DDQN [15], DQN [11], ALG-B [16], LSTM-WLS [17], and the proposed DQN-WLS. The implementation of all six algorithms, including network configurations and simulation parameters, is available for reproducibility.<sup>1</sup>

### B. Convergence Behavior

Fig. 2 reports the learning curves of PPO, DDQN, DQN, and the proposed DQN-WLS. The proposed DQN-WLS converges stably and achieves the lowest positioning error among the evaluated DRL baselines, benefiting from the geometry-consistent WLS refinement.

### C. Positioning Visualization

Fig. 3 compares ALG-B, DQN, and the proposed DQN-WLS at Episode 1000. The proposed DQN-WLS closely matches the ground truth and achieves sub-meter accuracy (0.395 m RMSE), while ALG-B and DQN exhibit much larger deviations.

### D. Performance Comparison

Table I summarizes the overall computational and localization performance of six representative algorithms, including both geometric and learning-based approaches. The conventional beam-intersection method (ALG-B [16]) exhibits the largest localization deviation ( $> 3 \text{ km}$ ) due to its reliance on fixed beam footprints without adaptive weighting. Among DRL-based schemes, PPO [14] and DDQN [15] incur substantially higher runtime under the considered training configuration, while the standard DQN [11] improves efficiency and reduces the positioning error to 10.38 m. The LSTM-WLS [17] framework achieves extremely high accuracy (0.01 m) but incurs high training cost and longer inference latency, making it impractical for real-time onboard operation. By contrast, the proposed DQN-WLS achieves sub-meter accuracy (0.395 m) with the lowest runtime (9.43 s per episode) and nearly identical computational complexity to DQN ( $\approx 19 \text{ GFLOPs}$ ). These results confirm that the proposed DQN-WLS achieves a favorable accuracy–efficiency trade-off with low per-step complexity. In addition, we include an ablation where  $\Delta f_{D_i} = 0$  (Doppler-free) and observe only a negligible RMSE change in our considered setting, indicating that the proposed method is robust under typical residual Doppler after compensation.

<sup>1</sup>Source code and configuration files are available at: [github.com/BoneZhou/DRL-LEO-Beam-Positioning](https://github.com/BoneZhou/DRL-LEO-Beam-Positioning)

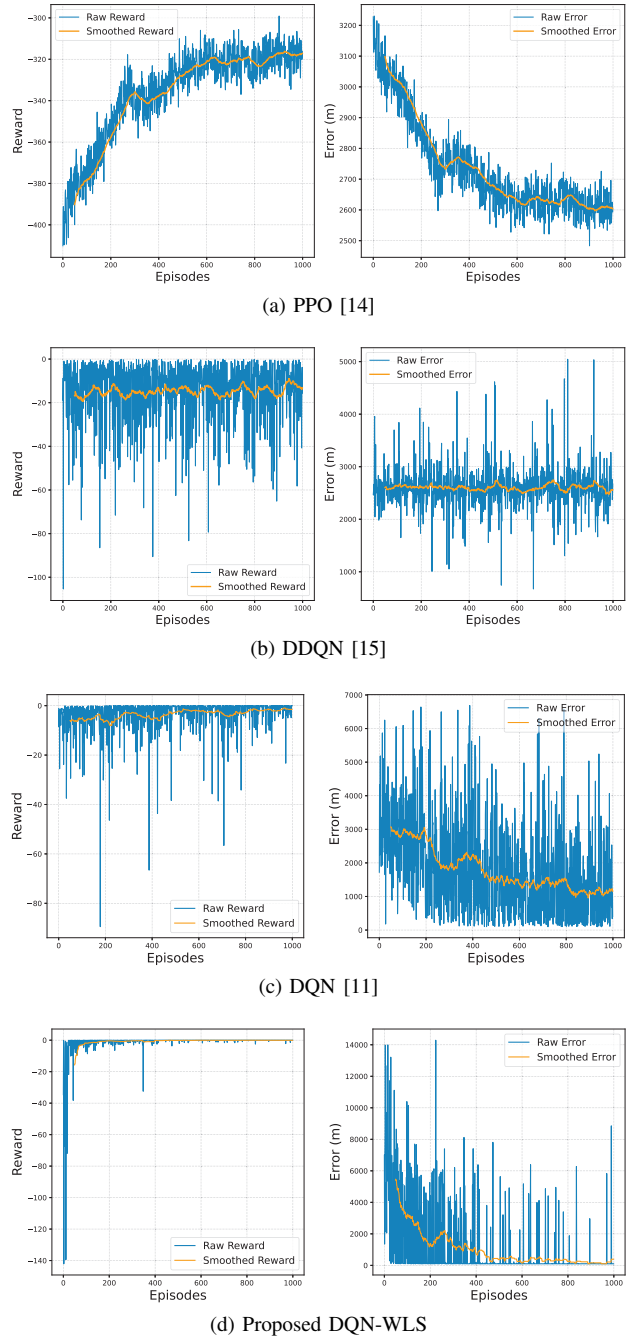


Fig. 2: Training convergence of cumulative reward and positioning error for PPO, DDQN, DQN, and the proposed DQN-WLS.

*Note:* Time and RMSE are averaged over 10 seeds under identical settings.

### E. Discussion

The favorable accuracy-runtime trade-off of DQN-WLS stems from its hybrid structure, combining the adaptivity of reinforcement learning with the stability and interpretability of model-based estimation. Through interaction with the environment, the agent learns to emphasize high-SINR and geometrically informative beams while suppressing noisy or redundant

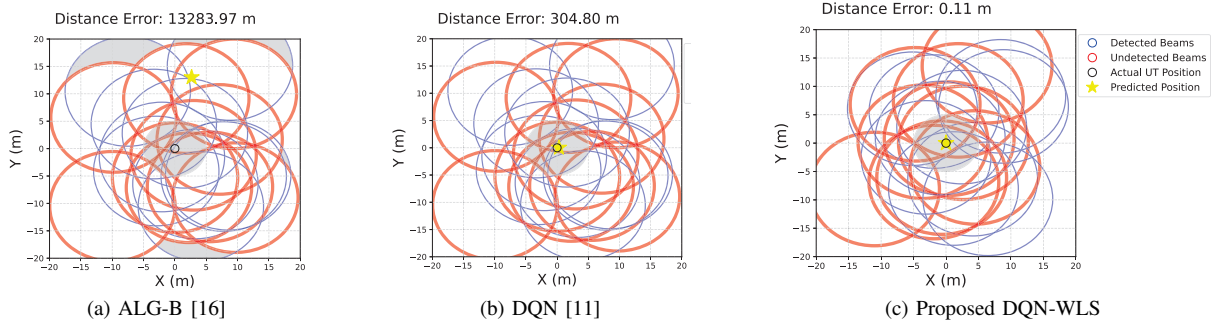


Fig. 3: Positioning visualization at Episode 1000 under identical satellite geometry and noise conditions. The yellow star denotes the estimated UT position, and the black circle indicates the ground truth. Compared with the geometry-driven ALG-B and standard DQN, the proposed DQN-WLS aligns closely with the ground truth and yields the smallest residual error.

TABLE I: Comparison of Positioning and Learning-Based Methods

Method	FLOPs (M)	Total FLOPs (G)	Time (s)	RMSE (m)
ALG-B [16]	–	–	2.61	3688.14
PPO [14]	0.07	92.87	3016.02	2558.33
DDQN [15]	0.04	77.59	350.08	2504.05
DQN [11]	0.02	18.94	13.52	10.38
LSTM-WLS [17]	31.24	78.09	262.96	<b>0.01</b>
Proposed DQN-WLS	0.02	18.95	<b>9.43</b>	<b>0.395</b>

ones, and the augmented WLS solver enforces geometric consistency during localization. We also include supervised LSTM-based weighting (LSTM-WLS [17]) as a reference that targets accuracy-optimal estimation in its supervised setting. In contrast, the proposed DQN-WLS is designed for CSI-free and deployment-oriented operation with low runtime overhead, which is relevant to resource-constrained LEO payload scenarios.

## VI. CONCLUSION

This paper investigated a DQN-WLS framework for CSI-free multi-satellite positioning in LEO constellations that learns discrete satellite-weighting policies from pilot-level observations and geometric features. By coupling a lightweight DQN policy with an augmented WLS estimator, the proposed method provides a deployment-oriented accuracy-runtime trade-off and preserves physics-consistent localization with clock-bias estimation. Simulation results in representative settings demonstrate sub-meter accuracy with low computational overhead, suggesting that hybrid RL-WLS designs are a promising direction for CSI-free beam-based positioning in NTN. Extending the framework to broader beam counts, richer interference models, and more diverse geometries is a natural next step.

## REFERENCES

- [1] S. Saleh, P. Zheng, X. Liu, H. Chen, M. F. Keskin, B. Priyanto, M. Beale, Y. Etefagh, G. Seco-Granados, T. Y. Al-Naffouri, and H. Wymeersch, “Integrated 6G TN and NTN localization: Challenges, opportunities, and advancements,” *IEEE Commun. Standards Mag.*, vol. 9, no. 2, pp. 63–71, 2025.
- [2] J. Zhu, Y. Sun, and M. Peng, “Beam management in LEO satellite networks with random traffic arrival and time-varying topology,” *IEEE Trans. Veh. Technol.*, vol. 73, no. 9, pp. 13352–13367, Sept. 2024.
- [3] Y. Cao, S.-Y. Lien, Y.-C. Liang, and D. Niyato, “Toward intelligent non-terrestrial networks through symbiotic radio: A collaborative deep reinforcement learning scheme,” *IEEE Netw.*, vol. 39, no. 1, pp. 211–219, 2025.
- [4] Z. Lin, Z. Ni, L. Kuang, C. Jiang, and Z. Huang, “Multi-satellite beam hopping based on load balancing and interference avoidance for NGSO satellite communication systems,” *IEEE Trans. Commun.*, vol. 71, no. 1, pp. 282–295, Jan. 2023.
- [5] J.-H. Lee, C. Park, S. Park, and A. F. Molisch, “Handover protocol learning for LEO satellite networks: Access delay and collision minimization,” *IEEE Trans. Wireless Commun.*, vol. 23, no. 7, pp. 7624–7637, July 2024.
- [6] H. Xu, Y. Sun, Y. Zhao, M. Peng, and S. Zhang, “Joint beam scheduling and beamforming design for cooperative positioning in multi-beam LEO satellite networks,” *IEEE Trans. Veh. Technol.*, vol. 73, no. 4, pp. 5276–5287, Apr. 2024.
- [7] A. Schröder, S. Gracla, M. Röper, D. Wübben, C. Bockelmann, and A. Dekorsy, “Flexible robust beamforming for multibeam satellite downlink using reinforcement learning,” in *Proc. IEEE Int. Conf. Commun. (ICC)*, June 2024, pp. 3809–3814.
- [8] Y. Wang, Y. Chen, Y. Qiao, H. Luo, X. Wang, R. Li, and J. Wang, “Cooperative beam hopping for accurate positioning in ultra-dense LEO satellite networks,” in *Proc. IEEE Int. Conf. Commun. Workshops (ICC Wkshps)*, June 2021, pp. 1–6.
- [9] A. Farajzadeh, A. Yadav, and H. Yanikomeroglu, “Federated learning in NTN: Design, architecture, and challenges,” *IEEE Commun. Mag.*, vol. 63, no. 6, pp. 26–33, 2025.
- [10] S. M. Kay, *Fundamentals of Statistical Signal Processing, Volume I: Estimation Theory*. Prentice Hall, 1993.
- [11] V. Mnih *et al.*, “Human-level control through deep reinforcement learning,” *Nature*, vol. 518, no. 7540, pp. 529–533, 2015.
- [12] E. D. Kaplan and C. J. Hegarty, *Understanding GPS/GNSS: Principles and Applications*, 3rd ed. Norwood, MA, USA: Artech House, 2017.
- [13] R. Shafin, L. Liu, Y. Li, Y. Li, A. Wang, and J. Zhang, “Angle and delay estimation for 3-D massive MIMO/FD-MIMO systems based on parametric channel modeling,” *IEEE Trans. Wireless Commun.*, vol. 16, no. 8, pp. 5370–5383, Aug. 2017.
- [14] J. Schulman, F. Wolski, P. Dhariwal, A. Radford, and O. Klimov, “Proximal policy optimization algorithms,” *arXiv preprint arXiv:1707.06347*, 2017.
- [15] H. van Hasselt, A. Guez, and D. Silver, “Deep reinforcement learning with double Q-learning,” in *Proc. AAAI Conf. Artif. Intell.*, Feb. 2016, pp. 2094–2100.
- [16] M. Elsanhoury, J. Koljonen, M. Elmusrati, and H. Kuusniemi, “A novel beam-based positioning paradigm via opportunistic signal of future massive MIMO LEO satellite constellations,” in *Proc. IEEE Int. Conf. Localization and GNSS (ICL-GNSS)*, Antwerp, Belgium, 2024, pp. 1–5.
- [17] I. Sbeity, C. Villien, C. Combettes, B. Denis, E. V. Belmega, and M. Chafii, “A novel satellite selection algorithm using LSTM neural networks for single-epoch localization,” in *Proc. IEEE/ION Position, Location and Navigation Symp. (PLANS)*, Monterey, CA, USA, 2023, pp. 105–112.